24^{th} Symposium on Naval Hydrodynamics
Fukuoka, JAPAN, 8-13 July 2002

Wave Patterns and Minimum Wave Resistance for High-Speed Vessels

E. O. Tuck, D. C. Scullen, and L. Lazauskas
(The University of Adelaide, Australia)

ABSTRACT

Flow fields and wave patterns are computed in both the near and far field of a moving ship-like disturbance of small amplitude, using efficient routines for the 3D Havelock source. Classical thin-ship wave patterns can be computed for conventional ships, catamarans or submarines by this method, accurately and with extremely fine detail, in minutes on inexpensive desktop computers. Similar methods can be used for surface pressure distributions, modelling either hovercraft or planing vessels of small draft. In contrast to the thin-ship case, the ability to compute accurate near-field flows is essential to the solution process for a prescribed planing surface, which requires solution of an integral equation to determine the equivalent pressure distribution. Such pressure distributions can also be optimised to minimise wave resistance, from which follows a formally simpler design process for planing surfaces, where the shape of the surface is output rather than input.

INTRODUCTION

Objects of length L travelling steadily at speed U at or near a free surface under gravity g tend to make large waves if and only if the Froude number $F = U/\sqrt{gL}$ takes values of the order of 0.55. This is because their length is then about half of the transverse wavelength $2\pi U^2/g$, and (roughly) equal and opposite waves from bow and stern add together. At such speeds, wavemaking dominates over other physical processes, and its accurate prediction is critical.

Most conventional marine vessels travel much more slowly than this, since generation of large waves costs energy, and in that low-speed range (say $F < 0.35$) the tendency has been to assume that theoretical estimates of wavemaking are unreliable. Although this is to a certain extent true, it is also somewhat unreasonable to ask theory to predict a small effect in the presence of much greater (e.g. viscous) effects.

Some special marine vessels, e.g. hovercraft, also normally operate at speeds that involve little wavemaking, because the Froude numbers are high, e.g. $F > 1.3$. Again, hydrodynamic theory seems not to have a large role to play; such vessels at their design speeds are essentially airplanes in ground effect. However, they must accelerate through the large wavemaking range ("hump speed") in order to get to their higher design speed.

The present paper is concerned with speed ranges corresponding specifically to large wavemaking, mostly (say) $0.4 < F < 1.0$. In that range, theoretical prediction of waves and wave resistance is potentially valuable, much more so than is often appreciated. For example, Figure 1, taken from Tuck (1987), shows a comparison between computations based on Michell's (1898) thin-ship wave resistance theory and experiments of Chapman (1972), for a parabolic strut with beam/length ratio 0.15. This indicates quite remarkable agreement for $F > 0.4$, even though this is not a particularly thin body. Although there were no experimental results for $F < 0.4$, one might suspect that the relative accuracy in predicting the small waves made in that range would not be as good as it is for higher speeds.

Another example where one might expect good accuracy is for travelling pressure distributions of "small" magnitude, modelling hovercraft and potentially also planing surfaces or flat ships. Our interest in thin or flat ships is not only in their wave resistance, which is one measure of the wave energy in the far-field waves, but also in the actual wave elevation pattern itself, and then not only in the far field, but also in the near field close to the vessel.

We first discuss a mature computational tool for thin ships, extending Michell's (1898) theory in a number of directions, but with emphasis on efficient computation of a detailed and accurate wave pattern over a large region including the immediate neighbourhood of the vessel. A similar code is then discussed for the wave patterns of travelling pressure patches. The latter is potentially useful not only in a direct sense for vessels such as hovercraft, but also in an inverse sense for planing surfaces or

flat ships, whose hull shape is equated to the free-surface shape immediately beneath a patch of pressure.

One of our aims is to reduce or minimise wave resistance. We summarise here new results for pressure patches of minimum resistance at fixed total load, and give examples illustrating the corresponding near-field wave patterns, which are candidate hull shapes for planing surfaces. Interestingly, although optimal pressure distributions are necessarily fore-aft symmetric, this does not imply such symmetry of the near-field pattern, nor of the flat-ship hull, whereas the corresponding optimal thin-ship theory demands fore-aft hull symmetry.

We also provide discussion and preliminary results on the inverse problem, namely that of finding the pressure distribution corresponding to a given flat-ship hull. This is a very difficult computational task, and we are continuing to work on it. However, design of a pressure distribution for low wave resistance, followed by direct computation of the shape of the corresponding flat-ship hull, is a computationally simpler task which is already complete.

HAVELOCK SOURCES

The topic of this paper is detailed and accurate computation of steady flow fields, wave patterns and wave resistance, for bodies moving at constant speed U at or near a free surface under gravity g, in calm water of infinite depth. The bodies must be small in some sense, so that the free-surface condition can be linearised, and there are many examples of such bodies, including thin ships, catamarans, submarines, hovercraft and other types of surface-effect ships, planing surfaces or flat ships, etc.

Subject to the usual assumption of an inviscid incompressible fluid moving irrotationally, all such flows can be generated by distributions of Havelock sources, which are point sources in the presence of the free surface. The velocity potential of a unit Havelock source (Havelock 1917, 1928, Wehausen and Laitone 1962, p. 484) located at $(x, y, z) = (0, 0, \zeta)$ is

$$G(x,y,z;\zeta) = -\frac{1}{4\pi^2}\Re\int_{-\pi/2}^{\pi/2} d\theta \int_0^\infty dk \; e^{-ik(x\cos\theta + y\sin\theta)}\left[e^{-k|z-\zeta|} - \frac{k+k_0\sec^2\theta}{k-k_0\sec^2\theta}e^{k(z+\zeta)}\right] \tag{1}$$

with $k_0 = g/U^2$. The path of k-integration passes above the pole at $k = k_0\sec^2\theta$, so guaranteeing that waves occur only for $x > 0$. The first term inside the square bracket of (1) contributes the potential of an ordinary

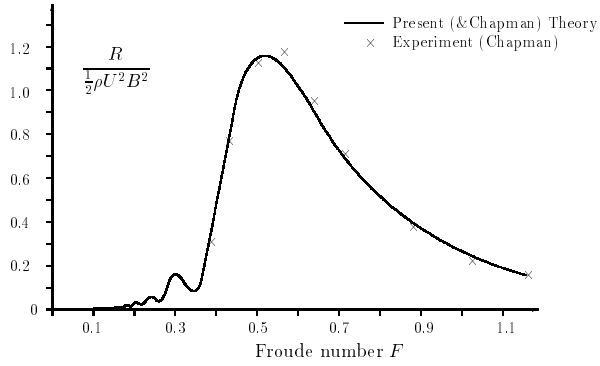

Figure 1: Comparison between theory and experiment for wave resistance of a parabolic strut.

infinite-fluid Rankine source, since

$$-\frac{1}{4\pi^2}\Re\int_{-\pi/2}^{\pi/2} d\theta \int_0^\infty dk e^{-ik(x\cos\theta + y\sin\theta) - k|z-\zeta|} = -\frac{1}{4\pi\sqrt{x^2+y^2+(z-\zeta)^2}}. \tag{2}$$

The second term inside the square bracket of (1) is the correction for the free surface, and it is easy to verify that the Kelvin linearised free-surface condition

$$G_{xx} + k_0 G_z = 0 \tag{3}$$

holds on $z = 0$.

Although the ability to represent free-surface flows by Havelock sources has been available for about a century, an apparent inhibition for routine use has been the sheer computational task of evaluating the double integral (1). When Havelock sources are distributed over a spatial region, at least two further numerical integrations have to be performed, and if detailed flow fields are then required at many (x, y, z) values, some *billions* of values of G may be required! There is therefore a premium on efficient evaluation of this double integral.

Newman (1987) made a significant advance in this direction by providing economised polynomial approximations for the "local" portion of the Havelock source, namely

$$G^L(x,y,z;\zeta) = G(-|x|,y,z;\zeta)\ . \tag{4}$$

This is an even function of x which is identical to G when $x < 0$, i.e. ahead of the source, and so is not wave-like. Thus $G = G^L + G^F$ where the "far-field" portion G^F is identically zero for $x < 0$, and for $x > 0$ is given by $-2\pi i$ times the residue at the pole, namely

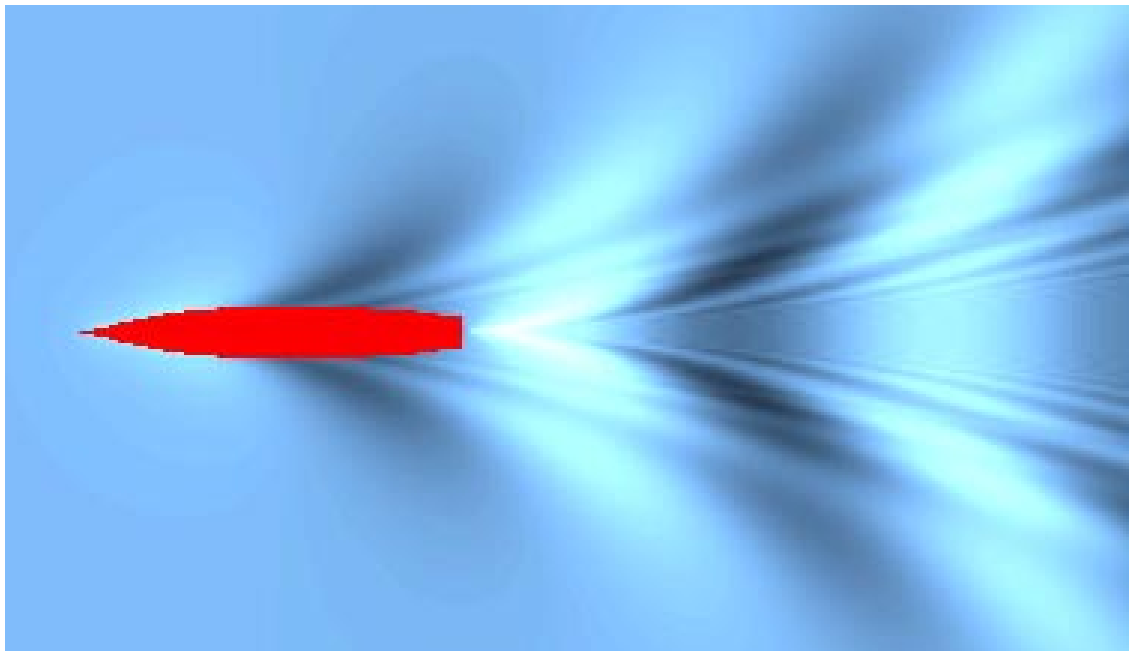

Figure 2: Computed wave pattern for a DDG51 ship at 30 knots.

$$G^F(x,y,z;\zeta) = -\frac{k_0}{\pi}\int_{-\pi/2}^{\pi/2} \sec^2\theta e^{k_0(z+\zeta)\sec^2\theta} \sin(k_0 x\sec\theta)\cos(k_0 y\sec^2\theta\sin\theta)\,d\theta\ . \quad (5)$$

Although defined by "only" a single integral, the far-field part G^F of the Havelock source in fact presents greater computational difficulties than the local term G^L, because of the rapidly oscillating character of the integrand, especially when $|\theta|$ approaches $\pi/2$, i.e. for extreme diverging waves, and in practice it is best to avoid its direct computation.

THIN SHIPS

For a monohull thin ship with offsets $y = \pm Y(x,z)$, the disturbance velocity potential is generated by a distribution of Havelock sources over the centreplane R in $y = 0$, with strength according to Michell (1898) of magnitude $2UY_x(x,z)$ per unit area at the point $(x,0,z)$. Thus

$$\phi(x,y,z) = 2U\iint_R d\xi d\zeta\ Y_\xi(\xi,\zeta)\ G(x-\xi,y,z;\zeta). \quad (6)$$

If we write the Havelock source $G = G^L + G^F$ as above, we can then write correspondingly $\phi = \phi^L + \phi^F$. The double integral in (6) can be carried out by direct numerical quadrature for the local part ϕ^L, but for the far-field part ϕ^F we proceed indirectly, c.f. Noblesse (2001). In the following, let the draft of the ship be T and the x values at the extreme bow and stern be x_B and x_S respectively. Thus the region R is $x_B < x < x_S$ and $-T < z < 0$.

Substituting the integral representation (5) for G^F, we find

$$\phi^F(x,y,z) = -\frac{2Uk_0^2}{\pi}\int_{-\pi/2}^{\pi/2} d\theta\sec^3\theta\ e^{k_0 z\sec^2\theta}\cos(k_0 y\sec^2\theta\sin\theta)\big[P\cos(k_0 x\sec\theta) + Q\sin(k_0 x\sec\theta)\big], \quad (7)$$

where

$$P + iQ = \frac{1}{-ik_0\sec\theta}\int_{-T}^{0} d\zeta\int_{x_B}^{x_E} d\xi\ Y_\xi(\xi,\zeta)e^{ik_0\xi\sec\theta + k_0\zeta\sec^2\theta}\ , \quad (8)$$

and the end value x_E for the ξ-integration in (8) depends in general on the coordinate x.

If $x < x_B$, so we are observing the flow forward of the ship, then in effect $x_E = x_B$, which means that $\phi_F \equiv 0$. If $x > x_S$, so we are observing the flow aft of the ship, then $x = x_S$, so the integration range in (8) is the whole centreplane R, and $P+iQ$ is independent of x. Finally, if $x_B < x < x_S$, so we are observing the flow between the bow and stern stations, then $x_E = x$. This distinction occurs simply because the far-field portion G^F of the

Havelock source contributes only for stations ξ ahead of the observation point x.

So long as there is no transom, and $x > x_S$, integration of (8) by parts gives a simple formula for $P + iQ$ involving the actual hull offsets Y, namely

$$P + iQ = \iint_R Y(\xi, \zeta) e^{k_0 \zeta \sec^2 \theta + i k_0 \xi \sec \theta} \, d\xi d\zeta. \quad (9)$$

If there is a transom with $Y(x_S, \zeta) > 0$, or if $x_B < x < x_S$, there is an important extra contribution from the integrated part, which is included in our computations, but is not quoted here for simplicity.

In any case, given the offsets Y, the (ξ, ζ) double integral over the hull centreplane to determine $P + iQ$ can be done efficiently once and for all by numerical quadratures, the results being stored for subsequent use in the integral (7) for the far-field potential. This storage must be for a fixed set of values of θ, and so long as $x > x_S$, results can then be obtained by a single θ-integration with no further cost from the integrals over R, for as many (x, y, z) values as desired. If $x_B < x < x_S$, there is some further cost, as new values of $P + iQ$ must be computed for each new x, but this is not usually a large impost.

The actual free-surface elevation is $z = Z(x, y) = -(U/g)\phi_x(x, y, 0)$, and our main output is the wave pattern, in the form of contour plots of this quantity $Z(x, y)$. However, the wave resistance is also immediately available via (8) with $x_E = x_S$, namely

$$R_W = \frac{2}{\pi} \rho U^2 k_0^4 \int_{-\pi/2}^{\pi/2} \left[P^2 + Q^2\right] \sec^5 \theta \, d\theta \, , \quad (10)$$

which is Michell's (1898) wave resistance integral. Note that the task of evaluating the wave resistance R_W is equivalent to that of evaluation of just one wave elevation value $Z(x, y)$ in the far field; we compute millions of such values, in the near field as well as the far field.

Generalisations of thin-ship theory

Although developed initially by Michell (1898) for conventional ships, the above theory has somewhat more general applicability. Recall that the only essential approximation is that the vessel can be represented by a centreplane distribution of Havelock sources of strength proportional to the local hull slope. Thinness of the hull justifies this approximation, but this thinness need not be extreme, and for wave pattern purposes, relative errors appear to be comparable to the beam-to-length ratio (Tuck and Scullen 2002), so accuracies of within $\pm 10\%$ are to be expected for most ships.

Note that the only requirement for thinness is that the beam is small compared to the length; the draft is irrelevant (Tuck 1987). In particular, thin-ship theory applies as well to submarine vessels as it does to surface vessels. Indeed it usually performs even better, since the former usually have a lower beam/length ratio. For conventional submarines, thin-ship results can be computed up to and beyond the point where the vessel breaks the surface. These results remain in good agreement with "exact" nonlinear computations (Tuck and Scullen 2002) as the submergence is reduced, right up to the point where the latter inevitably fail due to incipient breaking.

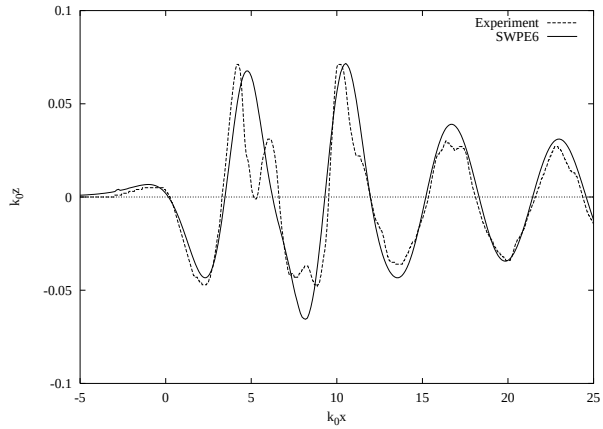

Figure 3: Comparison between SWPE computations for a ship model as in Figure 2 and "Wake-Off" experimental measurements along a cut parallel to the ship's track.

It is paradoxical (for both submerged and surface vessels) that the seemingly more accurate nonlinear theory, as implemented in Tuck and Scullen (2002) and in well-known codes such as RAPID (Raven 1996) and Shipflow (Larsson 1997), is nevertheless sometimes less useful because of the potential for such failure (see Abbott 1998 for a case study), than is the linear theory, which never fails numerically. Of course what the linear theory does in extreme cases is to predict one or two unreasonably large wave crests and deep troughs in the near field, which really should have broken. However, any such breaking is a highly localised phenomenon, and the wave pattern everywhere else and hence the wave resistance remain reasonable (Scullen and Tuck 1995).

Thin-ship theory also holds for multihull vessels, and again in most such cases the individual demihulls are thinner than conventional ships, so the linearisation is more justifiable. However, now there is a further complication involving interactions between hulls. In general, each demihull must be represented not only by centreplane distributions of Havelock sources, but also by centreplane distributions of lateral Havelock dipoles, the latter accounting for lateral velocities induced on one demihull by the others. In an aerodynamic analogy, this is a

"lifting" as distinct from a "thickness" effect (Newman 1977, p. 168), and also becomes relevant for a monohull at an angle of yaw (Xü 1991). There have been very few analyses of this type of interaction (see Lin 1974, Salvesen et al 1985, Suzuki et al 1997). However, the effect is expected to be quite small, and in particular is formally small if (as is usually the case) the demihulls are not only thin but also slender, i.e. have small draft/length ratio as well as small beam/length ratio (Tuck and Newman 1974, Tuck 1987). Its neglect enables consideration (Tuck and Lazauskas 1998) of optimal multihull arrangements to maximise cancellation of far-field waves and reduce wave resistance.

An apparent "generalisation" of thin-ship theory is to vessels with transom sterns. However, as long as the theory is applied with the source strength given in terms of hull slopes, e.g. use of (8) rather than (9), or a careful integration by parts is performed, the original Michell (1898) formulation is quite capable of handling dry transom sterns. This implies a representation of the subsequent trailing wake as a straight impermeable cylinder extending infinitely far downstream with cross-section identical to the transom. Somewhat better models of transom wakes are possible allowing eventual cavity collapse (Couser et al 1998, Doctors and Day 1997), but in practice the original Michell model works well.

A final generalisation is that of allowing viscous damping of the far-field waves. Since the far field can be considered as a superposition of plane waves travelling at angles θ to the x axis, with amplitude $P+iQ$, it is only necessary to apply appropriate damping factors to this plane wave (c.f. Lamb 1932, p. 624). We have found (Tuck et al 2002, c.f. Maruo 1976, equation (92); see also Cumberbatch 1965, Zilman and Miloh 2001) that the factor

$$\exp\left[-\frac{4\nu}{U}k_0^2\sec^5\theta(x\cos\theta+y\sin\theta)\right] \qquad (11)$$

inserted in the integrand of (7) provides good results, where ν is a measure of the kinematic viscosity. This quantity ν is not really intended to represent molecular viscosity as such, but to model the damping effect of the turbulent shear layer in the wake, and hence must take a value comparable to the eddy viscosity in the wake.

Choice of an appropriate value of ν is a difficult matter; a value of between 100 and 10000 times the molecular viscosity seems to eliminate some of the most extreme short diverging waves (with $|\theta|$ close to $\pi/2$) near the track of the ship, without unreasonably damping out genuine features of the wave pattern. Of course damping of far-field waves is not the only effect of viscosity, and for example it is also possible (Havelock 1948, Larsson 1997) to modify the source strengths to take account of apparent fattening of the hull due to the displacement thickness of the viscous boundary layer.

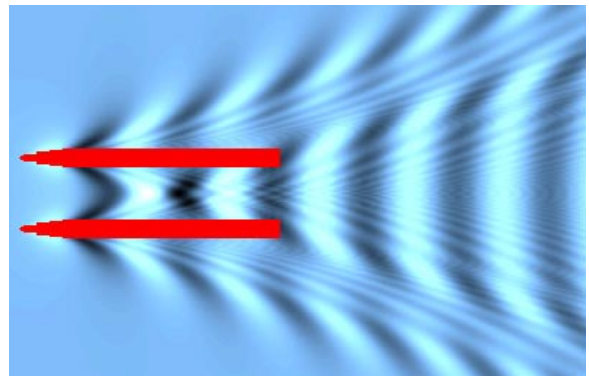

Figure 4: Computed pattern for a catamaran

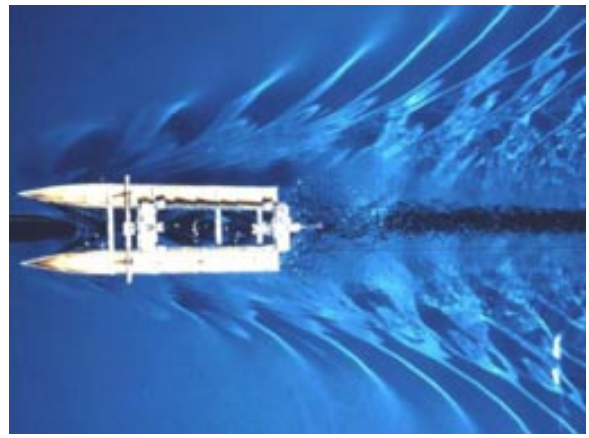

Figure 5: Photo of a catamaran model

Computational considerations

We have developed (Tuck et al 2002) a computer program "SWPE" which takes as input a conventional set of offsets defining the ship, and yields data suitable for plotting the resulting wave pattern over any specified region. A typical run of SWPE takes about fifteen minutes on a current PC to produce a detailed pattern containing about 100,000 points, yielding plots of photographic quality. One feature is the ability to "zoom" in arbitrarily close on any interesting flow region, although the mechanism for doing this is actually to re-sample by running SWPE again with the 100,000 points distributed over a smaller region, without loss of accuracy. In contrast, the resolution of "panel" methods (Raven 1996, Larsson 1997) is set in advance by the choice of the number and distribution of panels on the free surface, which is dictated by over-all accuracy requirements.

The similarity between (7) and (10) suggests that the triple (ξ,ζ,θ) numerical integration task of computation of the far-field potential ϕ^F at each separate point will

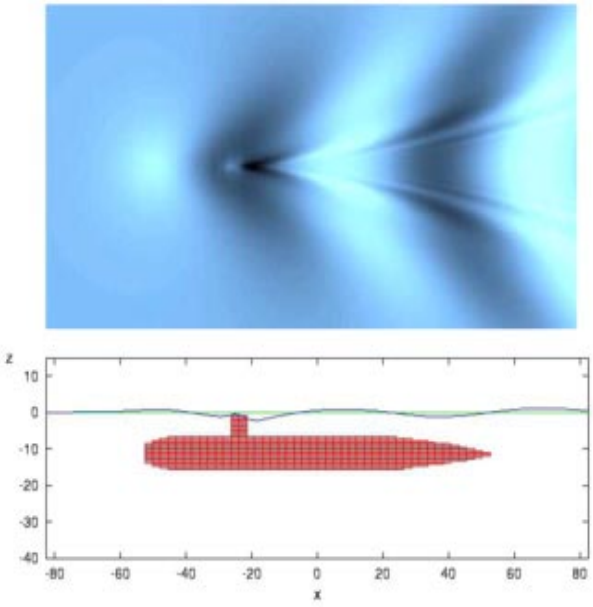

Figure 6: Wave pattern for a submarine.

be comparable to that of computing one value for the wave resistance R_W, already a daunting prospect if we desire information at 100,000 points or more, and made worse by the fourth k-integration needed for the local contribution ϕ^L to the potential.

We have previously (Tuck 1987, Tuck and Lazauskas 1999) developed efficient routines for evaluation of Michell's wave-resistance integral (10) subject to (8). These routines use Filon's (1926) quadrature (Abramowitz and Stegun 1964, p. 890) in the ξ-direction, in order to capture the rapid oscillations of the integrand of (8) as $|\theta| \to \pi/2$. Conventional (e.g. Simpson) quadratures fail to produce the correct rate of decay of the diverging part of the wave spectrum. That program computes the wave resistance of a typical ship to 4-figure accuracy in less than 50 milliseconds on an inexpensive 2GHz PC.

Essentially the same numerical methods that were successful for wave-resistance computations have been adapted in SWPE to compute the far-field flow and wave elevation. Again, Filon's quadrature plays an important role, and without it the diverging waves are poorly predicted. In addition, a special algorithm as in Tuck et al (1971) also captures the stationary-phase character of the integral (7) as $x, y \to \infty$, thus allowing uniform accuracy of computation as we move far away from the ship. The PC time to compute a single far-field point is then about 63 milliseconds. However, because the P, Q functions can be stored and used repetitively, the time to compute a wave field of 100,000 points is only about the same as for about 4000 separate single-point calculations, i.e. about 4 minutes.

It remains to compute the local portion $\phi^L(x, y)$, and in principle this remains a formidable quadruple-integration task. Fortunately, a significant part of this task has already been done for us, since Newman (1987) has provided economised polynomial approximations for G_L. Hence we need merely substitute this polynomial code into (6) and carry out the (ξ, ζ) integrations by Simpson's rule (no Filon treatment is needed as the local integrand is not rapidly varying). Nevertheless, one cannot entirely escape the fact that these computations require more arithmetic, and the local part of the computation tends to dominate computer times, typically by a factor of about four. The net effect is that the total PC time to compute a complete 100,000-point field is about 15 minutes.

Once such a field of wave elevations is computed, various plotting procedures can be used to display the results. We have found it convenient to use very finely graded contour plots. That is, we assign a colour (in the written paper gray, in the presentation blue) of varying intensity to each of a large but finite set of stepped levels of wave elevation Z. In practice we use 256 such levels, and with as many as 100,000 data points, the effect is close to what could be seen in a photograph taken vertically above the ship, although a careful examination of some Figures (especially where the elevation is relatively small) reveals evidence of actual discrete contours. We generally here delete information about the actual magnitude of these elevation contours, although this is available.

Sample results

Figures 2, 4 and 6 show respectively SWPE-computed wave patterns for a conventional ship, a catamaran, and a submarine. Other similar results are given in Tuck et al (2001) and Tuck (2001).

The ship in Figure 2 is in fact the same DDG51 destroyer hull as was used for the "Wake-Off" test (Lindenmuth et al 1991). As indicated in Figure 3, SWPE results for elevations along parallel cuts are in excellent qualitative and reasonable quantitative agreement with the experimental data. This agreement is somewhat better than was displayed by the various (then) state-of-the-art computer programs that participated in the 1991 Wake-Off test, and is comparable with that achieved subsequently by the very successful nonlinear code RAPID (Raven 1996). Some residual discrepancies are likely to be attributable to localised breaking in the experiments, which is unlikely to be capturable by any numerical code, linear or nonlinear.

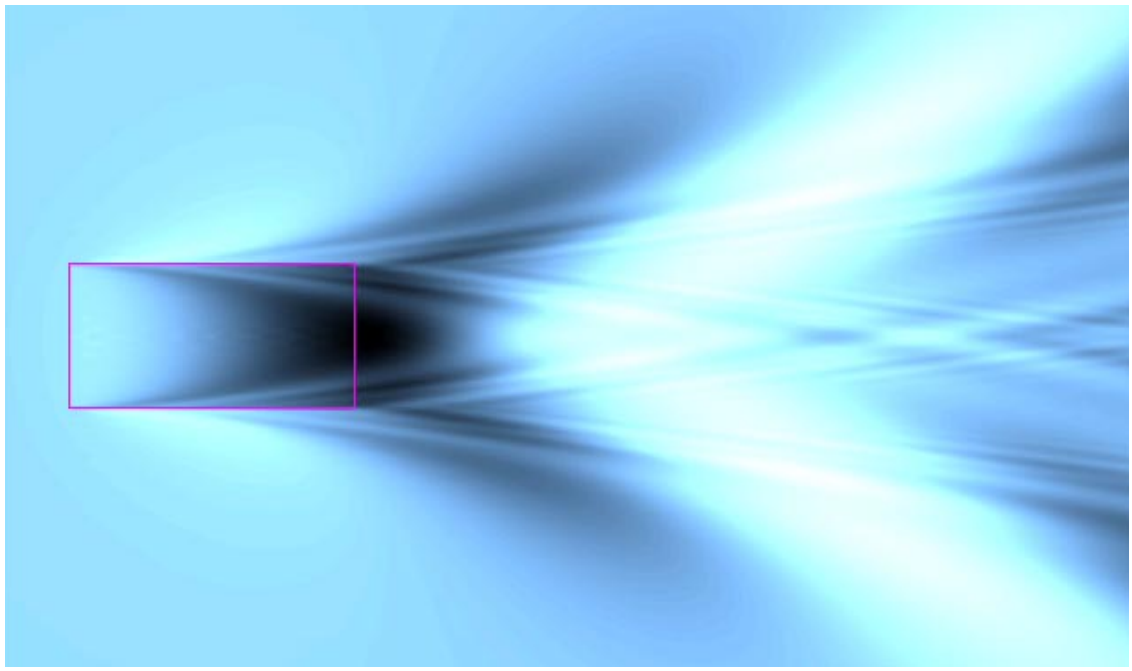

Figure 7: Constant-pressure patch.

Figure 4 provides SWPE computations for a catamaran hull, and can be compared to the photograph of Figure 5 (courtesy Australian Maritime College), although no attempt was made to duplicate the hull shape, and the speeds and dimensions were only roughly matched. There are obviously some points of close similarity, and also some features, mainly to do with the turbulent wake, that are not captured by the computations.

Figure 6 is for a Los Angeles class submarine hull moving at 10 knots, at a submergence such that the sail top is about to break surface. This pattern is especially interesting in that separate wave structures due to the sail and the main hull can be distinguished. The Froude number for the main hull is low enough for that part of the pattern to be mainly transverse, whereas the Froude number based on sail length is large, so that part of the pattern is mainly diverging.

PRESSURE DISTRIBUTIONS

The velocity potential for the flow induced by a unit delta-function pressure (Wehausen and Laitone 1962, p. 598) exerted on the free surface of a stream U is proportional to G_x, where $G(x, y, z; 0)$ is a Havelock source located at the free surface. That is, a pressure point is identical to a surface horizontal dipole. The velocity potential of a distribution of prescribed pressure $p(x, y)$ over a region R of the plane $z = 0$ is then

$$\phi(x, y, z) = \frac{U}{\rho g} \iint_R d\xi d\eta \; p(\xi, \eta) \; G_x(x-\xi, y-\eta, z; 0). \tag{12}$$

This is a similar formula to that (6) for a thin ship, the pressure distribution p replacing the offsets Y as input, but the region R is now part of the plane $z = 0$ instead of the plane $y = 0$. Again, separation into local and far-field portions enables direct computation of the local portion ϕ^L with the aid of Newman's (1987) representation for G^L, and indirect computation of the far-field portion ϕ^F proceeds in a similar manner to that for the thin ship. In particular, the same far-field potential (6) and wave-resistance formula (10) apply if we define

$$P + iQ = \frac{1}{2\rho U^2 k_0} \iint_R p(x, y) \; e^{ik_0 x \sec\theta + ik_0 y \sec^2\theta \sin\theta} dx dy. \tag{13}$$

The pressure-distribution version of our program SWPE computes the same set of wave-pattern and flow-field outputs as does the thin-ship version, with a simple replacement of the ship offset data $Y(x, z)$ at stations x and waterlines z, by pressure distribution data $p(x, y)$ at stations x and buttock lines y.

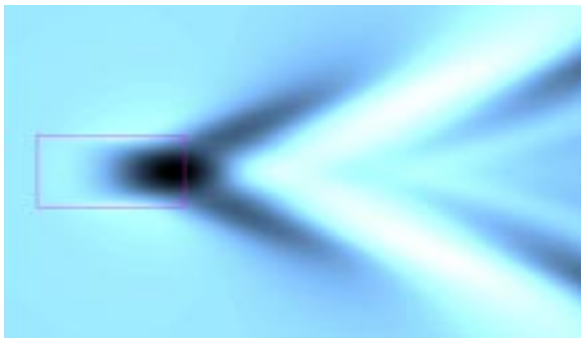

Figure 8: Single bi-quadratic pressure patch.

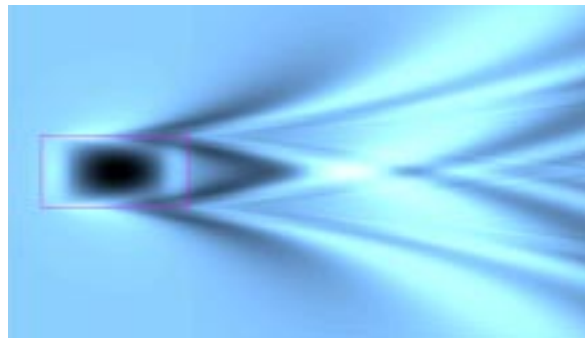

Figure 9: Wave pattern for tandem patches.

Results for simple pressure patches

All pressure-patch results in the present paper are for a rectangular region R, namely $|x| < a, |y| < b$. The results are parametrised with respect to the conventional length-based Froude number $F = U/\sqrt{2ga}$. We place special emphasis on a hovercraft-like beam/length ratio $b/a = 0.5$, and a Froude number $F = 1/\sqrt{2} \approx 0.7$, which is close to that (the so-called "hump speed", Everest and Hogben 1967) for maximum wave resistance.

Where necessary, as a specific example we have chosen a length $2a = 80$m, width $2b = 40$m and mean pressure $p_0 = 10$kPa, so the hydrostatic mean draft $z_0 = p_0/(\rho g)$ is about 1 metre and the displacement about 3200 tonnes. The hump speed U corresponding to $F = 1/\sqrt{2}$ is then about 40 knots; a real hovercraft of this size would normally travel at a greater speed where wavemaking is negligible, but we are more interested here in performance of a vessel of this size at a lower (but still high) speed where large waves are made unless there is some design optimisation.

The simplest type of pressure patch, of relevance to hovercraft, is one of uniform pressure $p = p_0 =$ constant over a rectangular region. The wave resistance of such patches was computed by Newman and Poole (1962, see also Doctors and Sharma 1972). Figure 7 shows the computed wave pattern for such a distribution.

Note the diverging wave structure, especially as it streams away from the step pressure discontinuity at the sides of the patch, which also induces a lateral step in the free-surface elevation. The step pressure discontinuity at bow and stern is of less significance from that point of view, c.f. Lamb (1932) p. 405, with a smooth continuous free surface. The present computational procedure is very efficient at displaying features such as these diverging waves, which have a very fine rapidly-varying structure that is hard to capture with "panel" methods, and this would be even more apparent in a view displaying more of the far field of the disturbance.

In the following it is convenient to define a non-dimensional wave resistance coefficent

$$C_D = \frac{\rho g R_W}{2bp_0^2}, \tag{14}$$

and for this special example, we have $C_D = 2.265$.

Because our numerical integration method has the accuracy of Simpson's rule for the integrals over R, it is almost exact for such uniform pressures, as well as for pressures that vary linearly or quadratically along or across the region.

Figure 8 shows the wave pattern for another example in this near-exact category, namely that for a "bi-quadratic" pressure

$$p(x,y) = \frac{9}{4}p_0 \left[1 - \left(\frac{x}{a}\right)^2\right] \left[1 - \left(\frac{y}{b}\right)^2\right] \tag{15}$$

which decays parabolically to zero at all sides of the patch. Here p_0 is the mean pressure, i.e. such that the lift $4abp_0$ is the same as that for a uniform pressure p_0. Although the bi-quadratic example of Figure 8 clearly yields a much smoother local wave field than the uniform pressure of Figure 7, it is far from being superior from the point of view of low (far-field) wavemaking, and has nearly double the wave resistance, namely $C_D = 4.270$.

However, there are certainly pressure distributions which perform much better from the wave-resistance point of view. One such is a tandem pair of patches.

For example, suppose there are two separate patches of positive pressure located at the bow and the stern, each occupying 20% of the overall length. Each patch is of bi-quadratic form, with a pressure similar (on its own planform) to that in (15), and the remaining 60% of the length between them is free of pressure. Figure 9 shows the resulting wave pattern. At fixed net lift, this configuration has $C_D = 1.330$, less than two-thirds of the wave resistance of the constant-pressure patch of Figure 7, and less than one-third of that of the full-length bi-quadratic patch of Figure 8. Figure 10 shows a perspective view of

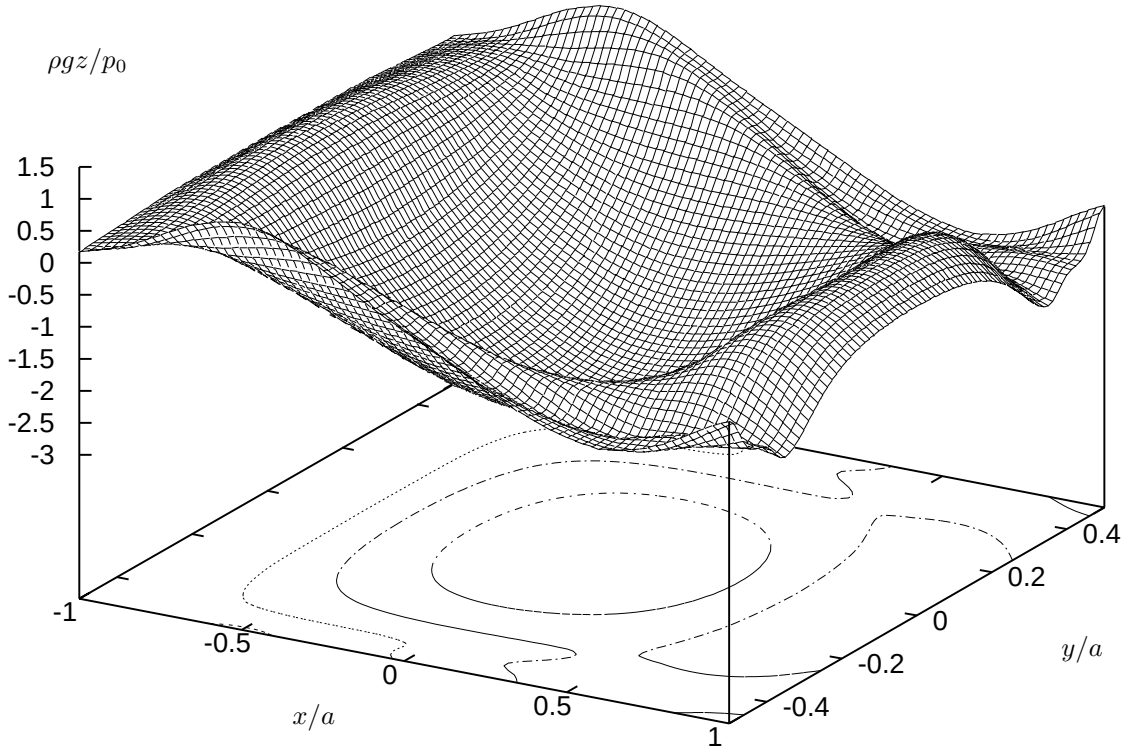

Figure 10: Elevation beneath the tandem pressures of Figure 9.

the elevation immediately beneath the planform R. The stern section has an appearance like a "tunnel" hull, an observation of relevance to use of this type of flow for design of planing surfaces. There is also an interesting comparison with optimised tandem hydrofoil configurations, e.g. as studied by Payne (1997).

Other examples are given in Scullen and Tuck (2002).

Minimum wave resistance patches

The above simple examples of pressure distributions are not necessarily optimal from the point of view of low wave resistance. Although for actual hovercraft there may be severe limitations on achievable pressure variations, nevertheless it is of significant interest to seek pressure distributions yielding minimum or at least low wave resistance, at fixed total lift force balancing the weight. This is not only of potential use for hovercraft, but also because such pressures might be achievable on the hull of a planing craft. That is, if we compute the wave elevation directly beneath such an optimised pressure distribution, the resulting free surface can be replaced by a solid surface, which would then represent a planing surface designed from the outset for low wave resistance.

Important early works on minimisation of wave resistance of travelling pressure distributions include those of Maruo (1949) and Bessho (1962). More recently Doctors (1997) (see also Doctors and Day 2000) has optimised unconstrained families of pressures, involving up to 4 distinct "subcushion" parameters, and we have (Tuck and Lazauskas 2001) optimised both unconstrained and constrained pressure distributions with many (e.g. 400) parameters, with indications of convergence toward a continuous optimum.

In the more practical case where the pressures are constrained to be non-negative, this continuous optimum has the following general structure, which varies with speed.

The most important feature (at all speeds where wavemaking is significant) is the presence of pressure lines of zero longitudinal extent concentrated at the extreme bow and stern ends. These end pressures vary in magnitude smoothly across the width, decreasing toward zero at the sides. In fact, an aerodynamic analogy (with exact equivalence between wave resistance and induced drag in the limit as $F \to \infty$) shows that at sufficiently high speed this lateral variation must be elliptic. However, at

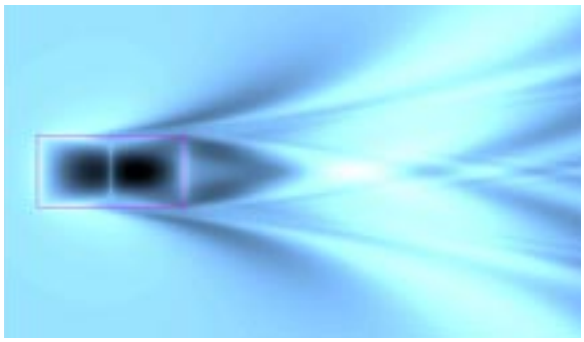

Figure 11: Wave pattern for optimum 3-line pressure.

beam/length ratio 0.5, we have found this to be so only for $F > 1.3$, with a preference for a more rapid decrease toward zero at the sides at lower speeds.

So long as $F > 0.96$ the optimum consists *only* of these two bow and stern pressure lines. Such Froude numbers are high enough that transverse wave cancellation by bow-stern interaction is ineffective, and the best that can be achieved is to place the disturbing pressures as far apart longitudinally as possible.

For $F < 0.96$ it is desirable to include a third patch of positive pressure, located midships. For $0.65 < F < 0.96$ the centre patch should also be of zero longitudinal extent, i.e. this patch is a pressure line similar to those at bow and stern. However, it should not in general extend all the way across the width of the rectangle, its optimal lateral extent varying in the range of 80% to 90% of the width.

As F decreases from 0.96, the centre patch bears an increasing fraction of the total load. For $F < 0.65$, the centre patch should have nonzero longitudinal extent, and by $F < 0.5$ it is essentially bearing the whole load, the end patches having withered away; however, by then the (minimised) wave resistance is quite small compared to that at the hump speed. We have little interest in optimum configurations at such low wave-making speeds.

In the present paper our main attention is paid to $F \approx 0.7$ and that is a speed where the optimum is three pressure lines, the central line being of about 85% of the full width, and bearing about 25% of the total load. This configuration has $C_D = 0.884$, and its wave pattern is shown in Figure 11. This is a very significant improvement on the constant-pressure result $C_D = 2.265$, and involves only physically-acceptable positive pressures.

Finally, if we do allow negative pressures, an even lower wave resistance is possible in principle, although the actual optimal pressures and the resulting elevations beneath the pressure patch are then not physically reasonable. We have (Tuck and Lazauskas 2001) used a 20 by 20 grid of rectangular constant-pressure panels, and find an optimum with the remarkably low wave resistance $C_D \approx 0.44$.

However, the price paid is quite large pressure variations, contours of pressure being as in Figure 12, with enormous maximum positive pressures of 275kPa (shown white) and minimum negative pressures of -160kPa (shown black). Figure 13 shows the resulting wave pattern. In this case, we display contours only for $|z| < 2$m, which captures all wave elevations outside the patch itself. However, inside the patch there are quite unrealistic troughs (shown black) of 37m and crests (shown white) of 26m! Clearly these unconstrained optima are mathematical curiosities only, and the requirement for non-negative optimal pressures is necessary in order for the results to be physically useful.

Free-wave spectrum

Some insight into the process of reduction of wave resistance for pressure patches is provided by the free-wave spectrum, which is proportional to $P^2 + Q^2$ where P, Q are defined by equation (13), and is a function of wave angle θ. Figure 14 presents graphs of the free-wave spectrum, here defined as $dR/d\theta$, where R is wave resistance. The vertical scale of the graph is irrelevant to the following discussion, but note that the area under each of the curves is proportional to the wave resistance R. Thus the free wave spectrum, in the form given here, immediately indicates those wave angles where most energy is shed.

For the single constant-pressure patch, the main peak in the free-wave spectrum occurs at about $\theta = 53^\circ$. A sensible wave-minimisation strategy would be to reduce this large peak. Clearly the bi-quadratic pressure distribution fails miserably in this regard. It has a large peak at about $\theta = 60^\circ$, which is more than double that of the constant-pressure patch, and it is no surprise that its wave resistance is also about double. Its edge smoothness results in a much lower envelope of the spectral peaks of the extreme diverging waves with $\theta > 75^\circ$, but these carry little energy.

The other pressure distributions shown in Figure 14 have a local minimum in their free-wave spectrum curves at wave propagation angles a little higher than that at which the constant-pressure patch reaches its peak. For $\theta < 35^\circ$, the tandem and the three-line pressures shed about 30% less energy than the constant-pressure case, and the pressure strips at the bow and stern provide a significant degree of cancellation of transverse waves. For $35^\circ < \theta < 60^\circ$, the energy lost to the diverging wave pattern is considerably less than for constant pressure.

The ultimate reduction in wave-making is evident from the curve for the unconstrained 20×20 optimum, which makes very low transverse waves, but also sheds

almost negligible energy in the range $40^\circ < \theta < 65^\circ$, whereas its spectral peaks for extreme diverging waves with $\theta > 75^\circ$ are higher than those of the other examples in Figure 14.

Similar methods of analysis were used by Tuck and Lazauskas (1998) to examine wave cancellation effects of multi-hulled displacement vessels.

PLANING SURFACES

Planing surfaces are flat ships, i.e. ships of small draft. However, unlike thin ships, for which the limiting solution as the beam goes to zero is explicit (as a quadruple integral) given the ship offsets, for flat ships we must still, even in the limit as the draft goes to zero, solve an integral equation over the wetted planform R. This integral equation is of a particularly unpleasant character in three dimensions (Maruo 1967, Tuck 1975), essentially because of short diverging waves which tend to induce unwanted oscillations. Early attempts to solve it numerically include those of Oertel (1975) and Doctors (1975), and good results have recently been obtained by Cheng and Wellicome (1994) and by Lai and Troesch (1995). The corresponding two-dimensional problem is much more straightforward, and has a large literature, partly surveyed in Tuck (1990). At the other extreme, for planing surfaces of low aspect ratio there have also been some explicit high Froude number solutions, e.g. Tulin (1957), Casling (1978), and Casling and King (1979).

In order to solve the three-dimensional planing-surface problem for a given flat ship with equation $z = Z(x, y)$, we "merely" need to find a pressure distribution $p(x, y)$ that causes the free surface to take that shape $z = Z(x, y)$ beneath the region R of non-zero pressure. The above examples of solutions of the direct problem when R is a rectangle are already in principle solutions of the planing surface problem, providing $Z(x, y)$ takes one of the output forms in the Figures. However, it is potentially a much more difficult task to invert this problem, thus finding p when Z is given.

Since the relationship between pressure and wave pattern is a linear one, formally this inversion only requires inversion of the linear operator. More concretely, if we discretise the pressure data $p(x, y)$ into a vector $\mathbf{p}$ of length N, and the free-surface elevation data $Z(x, y)$ into a vector $\mathbf{Z}$ of length M, our computer code provides a connection (implicitly or explicitly) of the form

$$A\,\mathbf{p} = \mathbf{Z} \tag{16}$$

for some $M \times N$ matrix A.

One possibility is that $M = N$, so that we compute exactly as many elevations as there are pressures. It is convenient to assume then that the elevations Z are computed at the same N nodal points within the planform R

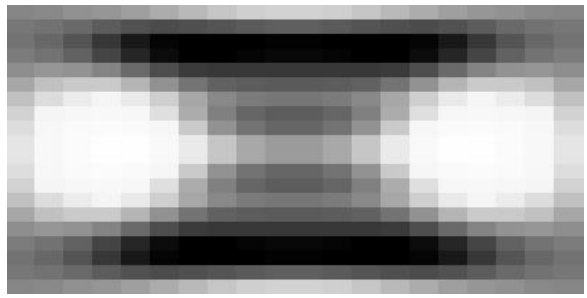

Figure 12: Unconstrained optimum pressure.

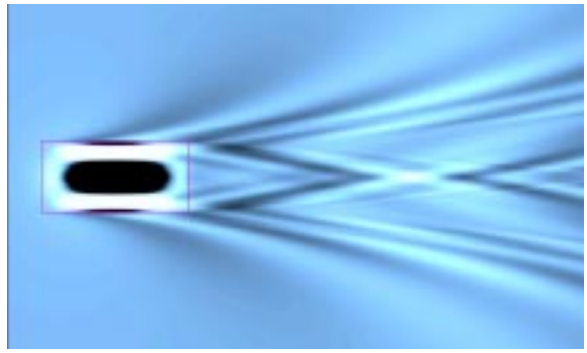

Figure 13: Wave pattern for unconstrained pressure.

as those where the pressures p are specified. Then the matrix A is square and $N \times N$, and it is only necessary that this matrix A be nonsingular (which it is) in order that we be able to find $\mathbf{p}$, given $\mathbf{Z}$.

It is also possible to perform an inversion if $M > N$, e.g. by using least squares. In that case we no longer demand that the pressure $p(x, y)$ exactly reproduce a given elevation $Z(x, y)$ at M points, but rather that the values of p at N points be such as to minimise the sum of the squared departures of the computed Z from the given elevations at M points. This leads to equations of the form

$$A^\top A\,\mathbf{p} = A^\top \mathbf{Z} \tag{17}$$

which can be solved by inversion of the $N \times N$ square matrix $A^\top A$. Use of $M >> N$ is desirable in that it averages out effects like the short diverging waves that have always caused numerical difficulties in this problem.

Edge conditions

There is an extra complication for actual planing surfaces, in that we must demand smooth detachment at the trailing end of the surface. That is, we only accept pressure distributions $p(x, y)$ which vanish (return to atmospheric pressure) at the trailing end of the planing

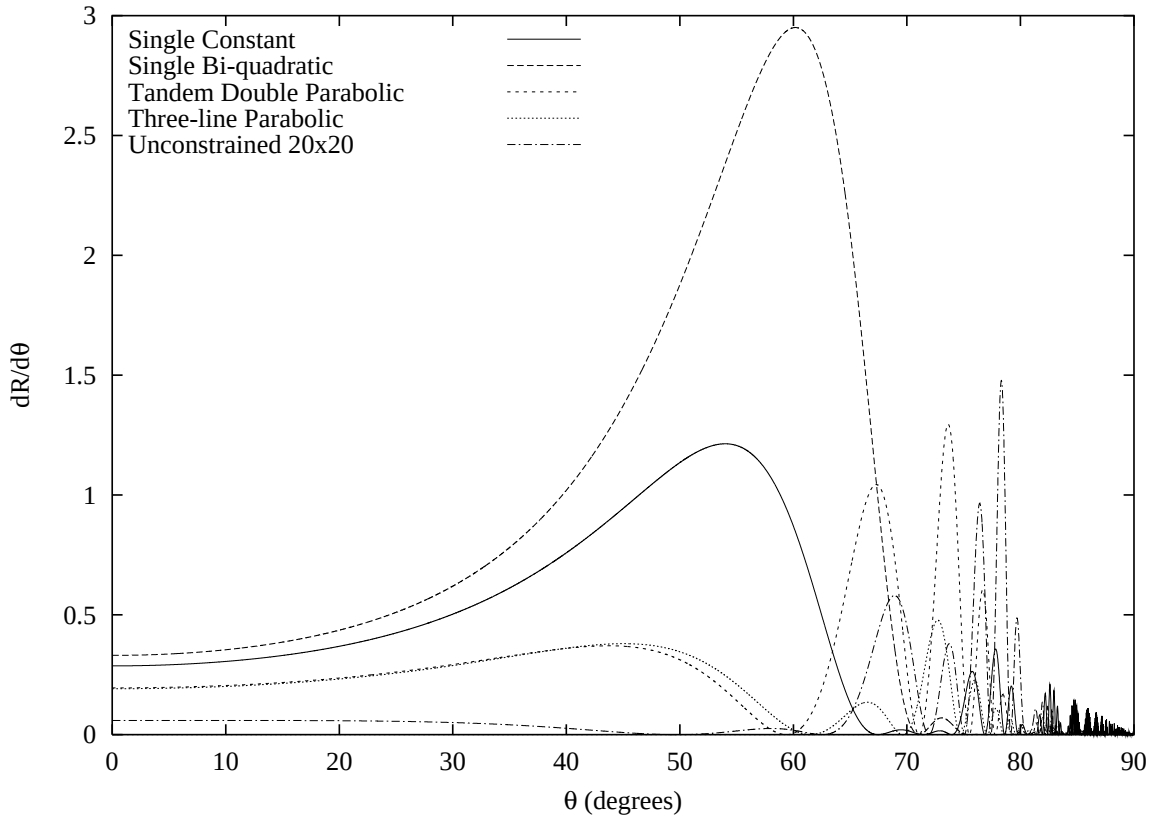

Figure 14: Free wave spectrum for various arrangements of pressure patches.

surface. This condition is referred to as a Kutta condition, by analogy with that (Newman 1977, p. 164) for lifting surfaces. The linear two-dimensional version of this planing-surface problem is similarly analogous (Tuck 1990, Bessho 1994) to thin-airfoil theory.

There is a price to pay for such an extra demand, since for any given $Z(x, y)$ we cannot expect the Kutta condition to hold upon direct inversion. There are two ways to pay that price. The most computationally straightforward way is, while retaining a fixed given planform R, to allow a degree of freedom in specification of $Z(x, y)$, e.g. a vertical shift $Z = Z_0(x, y) + C(y)$ where Z_0 is the given hull and $C(y)$ must be determined by the program. Thus the actual given hull shape is not preserved, but is "bent" about a longitudinal axis, which may not be acceptable for applications to real hulls.

Alternatively, and potentially more practically, we can allow a degree of freedom in specification of the wetted domain or planform R, while retaining on that new domain the exact given hull $Z = Z_0$. In practice, with a fixed trailing edge, this is normally an adjustment in the location of the leading edge, and such significant leading-edge adjustments are natural and inevitable for real planing surfaces. However, this is a computationally difficult task, and is not attempted in the present paper.

In general, having demanded zero pressure at the trailing edge, the leading-edge pressure will not only not vanish, but will formally become unbounded within the present linearised theory. This leading-edge singularity is again analogous to the corresponding leading-edge singularity (Newman 1977, p. 168) in aerodynamic lifting-surface theory. In the latter case, this is an artefact associated with rapid velocities at which fluid passes from the lower to the upper surface of a lifting wing, but in the planing-surface case it models a splash (Wagner 1932, Tuck 1994, 1995).

Since splashes contribute to the total drag, there is a premium on reducing or even eliminating this leading-edge singularity, and thus seeking pressures that vanish not only at the trailing edge but also at the leading edge. We then would need another degree of freedom, e.g. we may wish to modify the original hull Z_0 to

$$Z(x, y) = Z_0(x, y) + C_1(y) + xC_2(y) \ . \qquad (18)$$

This hull modification involves not only bending but also "twisting" the given hull about a longitudinal axis, with

an upshift $C_1(y)$ and an added angle of attack $-C_2(y)$ at each lateral position y, both determined by the program. This procedure generalises that of Cumberbatch (1958) to three dimensions and finite Froude number.

This does not end the list of possible constraints on the inversion task for planing surfaces. For example, we may consider it desirable to require the pressure to vanish along *all* of the boundary of the region R, not only at the leading and trailing edges, but also at the sides. This could be because (as seen in Figure 7 for the constant-pressure patch) sudden lateral terminations of the pressure tend to produce undesirable local diverging waves which may break, so producing further drag. It is also relevant that our work on minimisation of wave resistance suggests that optimal pressures tend to vanish at the sides.

For a rectangular planform R with side boundaries parallel to the stream, it is also not entirely obvious whether the side boundaries should be considered as "leading edges" or "trailing edges"; if the latter, we are required to demand a Kutta condition of zero pressure on them in any case. It is not hard to conceive of further degrees of freedom in modification of the original hull, allowing such a constrained inversion, but we leave that for future studies. Interestingly, Cheng and Wellicome (1994) seem to have been able to find solutions with zero side pressure without modifying the original hull for that purpose. One important feature noted by Tuck and Scullen (2002) is that when the side pressure steps from a finite value to zero, the free surface also steps by exactly the corresponding hydrostatic amount. Hence we cannot expect zero side pressure for bodies like flat plates where there is non-zero submergence at the sides.

This discussion about edge pressures highlights what is a serious numerical difficulty with the inversion problem for any planing surface, analogous with that for aerodynamic lifting surfaces, e.g. Tuck (1993). In general, such inversions (if performed exactly without discretisation) do not produce finite non-zero leading or trailing edge pressures. The edge pressure is either zero (e.g. when the Kutta condition is enforced) or infinite (e.g. at most leading edges). Hence when working with a discretised model, we must always in some sense be "approximating infinity". This difficulty can be overcome (see Tuck and Standingford 1997), but we must expect to see large numbers in the output pressures near edges, which can be accompanied by unacceptable grid-scale oscillations unless care is exercised in the numerical methods.

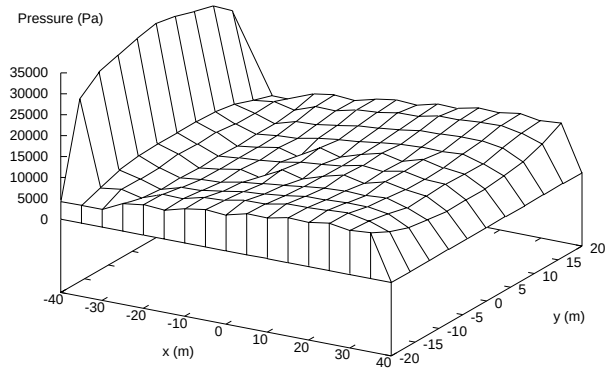

Figure 15: Pressure on flat plate

Flat plate example

In the present written paper we present just one example computation, for the input flat plate $Z_0(x, y) = -x/a$, with our standard rectangular planform and Froude number. This plate initially has its midship station $x = 0$ at the undisturbed free-surface level, with the bow raised to height 1m and the stern submerged to 1m. However, the program then generates an almost constant downshift, with $C(y) \approx -0.7$m, in order to satisfy the Kutta condition.

Figure 15 shows the resulting pressure distribution. The computations were performed by least squares, with $M = 2000$ input data points and $N = 176$ unknown pressures. The results are preliminary in that although the over-all trend and size of the pressure output is acceptable, small grid-scale oscillations are present, similar to those in other solutions such as those of Doctors (1975) and Cheng and Wellicome (1994). It is however notable that there is no indication of the pressure approaching zero at the sides of the plate, as assumed by Cheng and Wellicome (1994). Work is continuing on this challenging numerical task.

CONCLUSIONS

In this paper we have discussed three applications of linearised water-wave theory to efficient and accurate computation of flows and wave patterns for high-speed marine vessels. The first is a 21st-century computational realisation of the 19th-century thin-ship theory of Michell (1898). The resulting code is fast and accurate, and capable of revealing fine detail of the pattern that is difficult to capture by some other methods. In particular, its linearity conveys a number of advantages, not least of which is that it never fails.

The second application is to moving prescribed pres-

sure distributions, where again fine detail can be captured, in both near and far field. This fine detail includes, especially for distributions which do not vanish at the sides, very short diverging wave crests streaming away from corners and sides. Pressure distributions minimising wave resistance are also discussed and the importance of a non-negativity constraint is emphasised.

Finally, preliminary work on the inverse problem of finding a pressure distribution to match a given flat-ship hull is discussed. This is a notoriously difficult task, essentially because of the above-mentioned short diverging waves, and presents significant computational challenges. The present type of code shows considerable promise of yielding robust solutions, but we are not quite there yet.

ACKNOWLEDGEMENT

This work was supported by the Australian Research Council, and also by the Surveillance Systems Division of DSTO Australia. We thank Gregor McFarlane of the Australian Maritime College for Figure 5.

References

[1] Abbott, S. *An investigation into shallow water effects on high speed craft*, Thesis, Australian Maritime College, October 1998.

[2] Abramowitz, M. and Stegun, I.A., *Handbook of Mathematical Functions*, Dover, 1964.

[3] Bessho, M., "On the problem of the minimum wave-making resistance of ships," *Memoirs of the Defence Academy of Japan*, Vol. 2, 1962, pp. 1–30.

[4] Bessho, M., "On a consistent linearized theory of the wave-making of ships", *Journal of Ship Research*, Vol. 38, 1994, pp. 83–96.

[5] Casling, E.M., "Planing of a low-aspect-ratio flat ship at infinite Froude number", *Journal of Engineering Mathematics*, Vol. 12, 1978, pp. 43–57.

[6] Casling, E.M. and King G.W., "Calculation of the wetted area of a planing hull with a chine", *Journal of Engineering Mathematics*, Vol. 14, 1979, pp. 191–205.

[7] Chapman, R.B., "Hydrodynamic drag of semi-submerged ships", *ASME Journal of Basic Engineering*, 1972, pp. 874–884.

[8] Cheng, X. and Wellicome, J.F., "Study of planing hydrodynamics using strips of transversely variable pressure", *Journal of Ship Research*, Vol. 38, 1994, pp. 30–41.

[9] Couser, P.R., Wellicome, J.F., and Molland, A.F., "An improved method for the theoretical prediction of the wave resistance of transom-stern hulls using a slender body approach", *International Shipbuilding Progress*, Vol. 45, 1998, pp. 331–349.

[10] Cumberbatch E., "Two-dimensional planing at high Froude number", *Journal of Fluid Mechanics*, Vol. 4, 1958, pp. 466–478.

[11] Cumberbatch E., "Effects of viscosity on ship wakes", *Journal of Fluid Mechanics*, Vol. 23, 1965, pp. 471–479.

[12] Doctors, L. J., "Representation of three-dimensional planing surfaces by finite elements", *Proceedings of the 1st Conference on Numerical Ship Hydrodynamics*, Office of Naval Research, 1975, pp. 517–537.

[13] Doctors, L. J., "Optimal pressure distributions for river-based air-cushion vehicles", *Schiffstechnik*, Vol. 44, 1997, pp. 32–36.

[14] Doctors, L.J. and Day, A.H., "Resistance prediction for transom-stern vessels", *Fourth Int. Conf. on Fast Sea Transportation*, Sydney, 21–23 July 1997. Proceedings ed. N. Baird, Baird Publications, Melbourne, pp. 743–750.

[15] Doctors, L.J. and Day, A.H., "Wave-free river-based air-cushion vehicles". *Proceedings of International Conference on Hydrodynamics of High-Speed Craft Wake Wash and Motions Control*, London, November 2000.

[16] Doctors, L.J. and Sharma, S.D., "The wave resistance of an air-cushion vehicle in steady and accelerated motion", *Journal of Ship Research*, 1972, pp. 248–260.

[17] Everest, J.T. and Hogben, N., "Research on hovercraft over calm water", *Transactions of the Royal Institution of Naval Architects*, Vol. 109, 1967, p. 311.

[18] Filon, L.N.G., "On a quadrature formula for trigonometric integrals", *Proceedings of the Royal Society of Edinburgh*, Vol. 49, 1929, pp. 38–47.

[19] Havelock, T.H., "Some cases of wave motion due to a submerged obstacle", *Proceedings of the Royal Society of London*, Series A, Vol. 93, 1917, pp. 524–532.

[20] Havelock, T.H., "Wave resistance", *Proceedings of the Royal Society of London*, Series A, Vol. 118, 1928, pp. 24–33.

[21] Havelock, T.H., "Calculations illustrating the effect of boundary layer on wave resistance", *Transactions of the Royal Institution of Naval Architects*, Vol. 90, 1948, pp. 92–80.

[22] Lai, C. and Troesch, A.W., "Modelling issues related to the hydrodynamics of three-dimensional steady planing", *Journal of Ship Research*, Vol. 39, 1995, pp. 1–24.

[23] Lamb, H., *Hydrodynamics*, Cambridge, 1932.

[24] Larsson, L., "CFD in ship design – prospects and limitations," *Schiffstechnik*, Vol. 44, 1997, pp. 133–154.

[25] Lin, W.C., "The force and moment on a twin hull ship in steady potential flow", *Proceedings of the 10th Symposium on Naval Hydrodynamics*, ONR, Washington DC, 1974. pp. 493–516.

[26] Lindenmuth, W.T., Ratcliffe, T.J., and Reed, A.M., "Comparative accuracy of numerical Kelvin wake code predictions – 'Wake-Off' ". *David Taylor Research Center*, Report DTRC-91/004, Department of The Navy, Bethesda, MD, USA, 1991.

[27] Maruo, H., (in Japanese), *Journal of the Society of Naval Architects of Japan*, Vol. 81, (1949).

[28] Maruo, H., "High and low-aspect ratio approximation of planing surfaces", *Schiffstechnik*, Vol 72, 1967, pp. 57–64.

[29] Maruo, H., "Ship waves and wave resistance in a viscous fluid", *Proceedings of the 1st International Seminar on Wave Resistance*, Tokyo, February 1976.

[30] Michell, J.H., "The wave resistance of a ship." *Philosophical Magazine*, Series 5, Vol. 45, 1898, pp. 106–123.

[31] Newman, J.N., *Marine Hydrodynamics*, MIT Press, 1977.

[32] Newman, J.N., "Evaluation of the wave-resistance Green function: Part 1 – The double integral", *Journal of Ship Research*, Vol. 31, 1987, pp. 79–90.

[33] Newman, J.N. and Poole, F.A.P., "The wave resistance of a moving pressure distribution in a canal", *Schiffstechnik*, Vol. 9, 1962, pp. 1–6.

[34] Noblesse, F., "Analytical representation of ship waves" (23rd Weinblum Memorial Lecture), *Schiffstechnik*, Vol. 48, 2001, pp. 23–48.

[35] Oertel, R.P., "The steady motion of a flat ship, with an investigation of the flow near the bow and stern", Ph.D. Thesis, The University of Adelaide, 1975.

[36] Payne, P. , "On the maximum speed of the dynafoil", *Fourth Int. Conf. on Fast Sea Transportation*, Sydney, 21–23 July 1997. Proceedings ed. N. Baird, Baird Publications, Melbourne, pp. 283–290.

[37] Raven, H.C., "A solution method for the nonlinear ship wave resistance problem", Doctoral Thesis, Technical University Delft, 1996.

[38] Salvesen, N., von Kerczek, C., Scragg, C.A., Cressy, C.P. and Meinhold, M.J., "Hydrodynmamic design of SWATH ships", *Transactions of the Society of Naval Architects and Marine Engineers*, Vol. 93, 1985, pp. 325–348.

[39] Scullen, D.C. and Tuck, E.O., "Nonlinear free-surface flow computations for submerged cylinders", *Journal of Ship Research*, Vol. 39, 1995, pp. 185–193.

[40] Scullen, D.C. and Tuck, E.O., "Free-surface elevation due to moving pressure distributions in three dimensions", *Journal of Ship Research*, 2002.

[41] Suzuki, K., Nakata, Y., Ikehata, M., and Kai, H., "Numerical prediction on wave making resistance of high speed trimaran", *Fourth Int. Conf. on Fast Sea Transportation*, Sydney, 21–23 July 1997. Proceedings ed. N. Baird, Baird Publications, Melbourne, pp. 611–621.

[42] Tuck, E.O., "Low-aspect-ratio flat-ship theory", *Journal of Hydronautics*, Vol. 9, 1975, pp. 3–12.

[43] Tuck, E.O., *Wave resistance of thin ships and catamarans*, Report T8701, Applied Mathematics Department, The University of Adelaide, 1987. (downloadable from: http://www.maths.adelaide.edu.au/Applied/staff/etuck/).

[44] Tuck, E.O., "Planing surfaces", Chapter 7 of *Numerical Solution of Integral Equations*, ed. M. Golberg, Plenum Press, 1990.

[45] Tuck, E.O. "Some accurate solutions of the lifting surface integral equation", *ANZIAM Journal*, Vol. 35, 1993, pp. 127–144.

[46] Tuck, E.O., "The planing splash", *Proceedings of the 9th International Workshop on Water Waves and Floating Bodies*, Kuju, Japan, April 1994, ed. M. Ohkusu, Kyushu University, pp. 217–220.

[47] Tuck, E.O., "Planing surfaces", *Proceedings of the A.C. Aitken Centenary Conference*, Dunedin, N.Z., August 1995, ed. L. Kavalieris et al, University of Otago Press, 1996, pp. 331–340.

[48] Tuck, E.O., "Waves made by surface or underwater ocean vehicles", *Symposium on Ocean Survey and Resource Development Technology*, Proceedings ed. Han-il Park, Korea Maritime University, Busan, November 2001.

[49] Tuck, E.O., Collins, J.L. and Wells, W.H., "On ship waves and their spectra", *Journal of Ship Research*, 1971, pp. 11–21.

[50] Tuck, E.O. and Lazauskas, L., "Optimum spacing of a family of multihulls", *Schiffstechnik*, Vol. 45, 1998, pp. 180–195.

[51] Tuck, E.O. and Lazauskas, L., "Polymich", Department of Applied Mathematics, The University of Adelaide, 1999.

[52] Tuck, E.O. and Lazauskas, L., "Free-surface pressure distributions with minimum wave resistance", *ANZIAM Journal*, Vol. 43, 2001, pp. E75–E101.

[53] Tuck, E.O. and Newman, J.N., "Hydrodynamic interactions between ships", *Proceedings of the 10th Symposium on Naval Hydrodynamics*, ONR Washington DC, 1974, pp. 35–70.

[54] Tuck, E.O., Scullen, D.C. and Lazauskas, L., *Ship Wave Pattern Evaluation, Part 6 Report: Viscosity Factors*, The University of Adelaide, January 2002. (this and earlier SWPE reports are downloadable from: http:// www.maths.adelaide.edu.au/ Applied/staff/dscullen/).

[55] Tuck, E.O., Scullen, D.C. and Lazauskas, L., "Ship-wave patterns in the spirit of Michell", *Proceedings of the IUTAM Symposium on Free-Surface Flows*, Birmingham, July 2000, ed. A.C. King and Y.D. Shikhmurzaev, Kluwer Academic Publishers, Dordrecht, 2001, pp. 311–318.

[56] Tuck, E.O. and Scullen, D.C., "A comparison of linear and nonlinear computations of waves made by slender submerged bodies", *Journal of Engineering Mathematics*, 2002.

[57] Tuck, E.O and Standingford, D.W.F., "Numerical solution of the lifting surface equation", *Boundary Element Technology XII*, Knoxville, Tenn, 9–11 April 1997. Proceedings ed. J.I. Frankel, C.A. Brebbia and M.A.H. Aliabadi, Computational Mechanics Publications, Southampton, pp. 195–206.

[58] Tulin, M. P., "The theory of slender surfaces planing at high speeds", *Schiffstechnik*, Vol. 21, 1957, pp. 125–133.

[59] Wagner, H., "Über stoß- und Gleivorgänge an der Oberfläche von Flüssigkeiten", *Zeitschrifte angewandte Mathematik u Mechanik*, Vol. 12, 1932, pp. 1931–215.

[60] Wehausen, J.H. and Laitone, E.H., "Surface Waves", in *Handbuch der Physik*, ed. Flugge W., Ch. 9. Springer-Verlag, 1962.

[61] Xü, Hongbo, "Potential flow solution for a yawed surface-piercing plate", *Journal of Fluid Mechanics*, Vol. 226, 1991, pp. 291–317.

[62] Zilman, G. and Miloh, T., "Kelvin and V-wakes affected by surfactants", *Journal of Ship Research*, Vol. 45, 2001, pp. 150–163.